



Design of Crescent Splitting Electrodes in EWOD Device

Z. Wang, L. Chen[†] and X. Bian

Robotics & Microsystem Center & Collaborative Innovation Center of Suzhou Nano Science and Technology, Soochow University Suzhou 215123, China

†Corresponding Author Email: chenliguo@suda.edu.cn

(Received September 12, 2019; accepted February 3, 2020)

ABSTRACT

High control voltage and low success rate limit the application of droplet cutting on digital microfluidic chip, hence, the traditional square electrode was designed to crescent electrode to solve these problems in this paper. First, the relationship between the EWOD tension of micro-droplet and the chord length of effective Triple Contact Line (TCL) was analyzed based on the theory of electrowetting-on-dielectric. Then, the droplet cutting processes of different electrodes were numerically simulated and the results were analyzed. Finally, the effect of droplet cutting on four kinds of chips were tested. The results reveal that the crescent electrode can decrease the applied voltage for droplet cutting and the minimum voltage required for cutting on crescent electrode ($A=1.41$) was at least 13.9% lower than that of square electrode. In addition, the success rates of droplet cutting on crescent electrode at different channel heights are higher than that of square electrode.

Keywords: Electrowetting-on-dielectric; Digital microfluidics; Crescent electrode; Splitting voltage.

NOMENCLATURE

C	capacitance per unit area of the dielectric layer	V	driving voltage
F	surface tension force	θ_V	actuated contact angle
F_{EWOD}	EWOD tension along the effective TCL	θ_0	non-actuated contact angle
f_{er}	EWOD tension generated at each point	ϵ_r	dielectric constant of insulating layer
L	length of the chord formed by the effective TCL	ϵ_0	vacuum dielectric constant
P	pressure	γ_{lg}	liquid-gas surface tension,
t	thickness of insulator	\emptyset	level set function
TCL	Triple Contact Line	ρ	density
		μ	dynamic viscosity

1. INTRODUCTION

Microfluidic technology as a kind of technology that can operate micro-fluids is widely used in such fields as chemistry, biology and medicine (Jebrail *et al.* 2012; Shen *et al.* 2014; Choi *et al.* 2012). Generally speaking, this technology can be divided into continuous microfluidic and digital microfluidic. Compared with continuous

microfluidic, digital microfluidic realizes the selectivity of the path and effectively avoids contamination between liquids (Mark *et al.* 2010; Haerberle and Zengerle 2007; Fouillet *et al.* 2008). As the frontier of digital microfluidic, electrowetting-on-dielectric (EWOD) eliminates the need for complex equipment such as micro-pipes, micro-valves and micro-pumps to make droplet operations simpler and more flexible.

However, excessively high voltage will break the chip and damage the active substances carried in the droplet such as proteins and enzymes. Therefore, the applied voltage should be as low as possible. Several researchers have attempted to improve the on-chip cutting process. The geometry parameters of the chip including the spatial position of zero electrodes, the channel height, and the size of electrodes can be optimized to achieve low voltage (Samad *et al.* 2015; Jagath *et al.* 2017). In this paper, the influence of the shape of electrode on the voltage is studied. The effects of the voltage reduction of electrodes with different shapes are analyzed by numerical simulation and experiment.

2. THEORY

2.1 Droplet Cutting

Droplet cutting based on EWOD is typically completed on three square electrodes, as shown in Fig.1. Droplet was between the top and bottom plates, and when an electric potential is applied on both sides, charges on the surface of insulator modify the interfacial tension between the droplet and the insulator (Mugele & Baret, 2005). Then, the relationship between applied voltage and contact angle can be described by the Yang-Lipman equation:

$$\cos \theta_v - \cos \theta_0 = \frac{\epsilon_r \epsilon_0}{2\gamma_{lg}t} V^2 \quad (1)$$

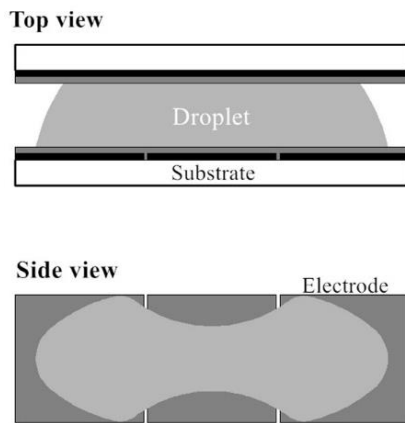


Fig. 1. Illustration of top and side view of EWOD device and droplet.

2.2 Voltage Reduction Principle

The shapes of the electrode in digital microfluidic chip include square and crescent, as shown in Fig. 2 (Rajabi *et al.* 2010). In order to verify the performance of crescent electrode, three different types of crescent electrodes were designed. The relationship between arc diameter D and W is:

$$A = \frac{D}{W} \quad (2)$$

The value A of three crescent electrodes are 3, 2, and 1.41, respectively.

The dotted circle is the contact circle of droplet. When the electric potential is applied to both electrodes, the horizontal EWOD tension generated at each point on the TCL is (Xu *et al.* 2014):

$$f_{er} = \frac{1}{2} cV^2 \quad (3)$$

Then, the horizontal EWOD tension along the effective TCL can be calculated by integrating:

$$F_{EWOD} = f_{er} \cdot L \quad (4)$$

It can be concluded from Eq. (4) that the EWOD tension is proportional to the L (Jong & James, 2011). Therefore, the larger the L , the greater the EWOD tension. Hence, the ideal EWOD tension can be obtained at a low voltage under the premise of increasing the L , thereby achieving the purpose of reducing the voltage.

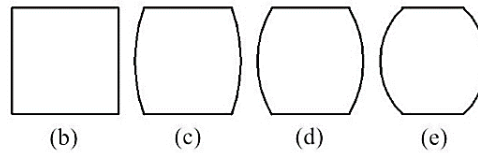
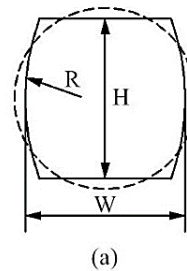


Fig. 2. Illustration of electrodes: (a) Cross section circle of electrode and droplet; (b) Square electrode; (c) Crescent electrode (Opposite layout, $A=3$); (d) Crescent electrode (Opposite layout, $A=2$); (e) Crescent electrode (Opposite layout, $A=1.41$).

Compared with square electrode, the spacing between the crescent electrode and the cross section outline of droplet is even, then the TCL of droplet diffuses more uniformly, and L is larger. The droplet can also be split successfully on the crescent electrode below the minimum voltage required for square electrode.

3. NUMERICAL TECHNIQUES

3.1 Level Set Method

We obtained the liquid-gas interface by capturing a zero level set of the function ϕ (level set function). In this paper, level set function ϕ satisfies the

following formula (Osher & Fedkiw, 2003):

$$\phi_t + \mathbf{V} \cdot \nabla \phi = 0 \quad (5)$$

The multiphase flow model, laminar two-phase flow and level set method were used in our simulation. The interface moves with the fluid velocity, \mathbf{V} . Then, the convection of the reinitialized level set function was given by (Olsson & Kreiss, 2005; Yue *et al.* 2004):

$$\phi_t + \mathbf{V} \cdot \nabla \phi + \gamma \left[\nabla \cdot \left(\phi(1 - \phi) \frac{\nabla \phi}{|\nabla \phi|} \right) - \varepsilon \nabla \cdot \nabla \phi \right] = 0 \quad (6)$$

Here, the parameter γ determines the amount of re-initialization and the thickness of the transition layer is proportional to ε .

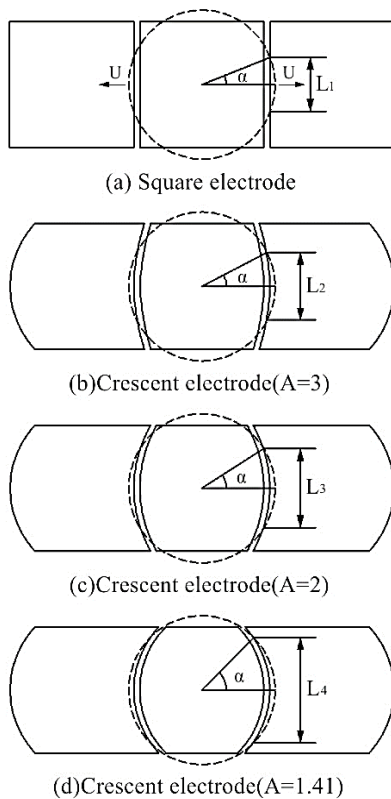


Fig. 3. Top view of the illustration of effective TCL.

3.2 Governing Equations of Liquid Flow

In this section, we made assumptions about the motion of droplet in EWOD device (Walker & Shapiro, 2006). Taking the liquid density and the relatively large spacing of the plates (i.e. the channel height is larger than a micron) into consideration, the flow was assumed to be a continuum (Karniadakis & Beskok, 2001) because the Knudsen number was very small. Incompressibility and Newtonian fluid assumptions may be used and NS equation is applicable (Panton, 1996):

$$\nabla \cdot \mathbf{V} = 0 \quad (7)$$

$$\rho(\mathbf{V}_t + \mathbf{V} \cdot \nabla \mathbf{V}) - \nabla \cdot (\mu(\nabla \mathbf{V} + \nabla \mathbf{V}^T)) + \nabla \mathbf{P} = \mathbf{F} \quad (8)$$

3.3 Boundary Conditions

The boundary conditions were used to achieve correct motion of droplets. The specific settings are as follows:

Walls

$$\mathbf{V} = 0 \quad (9)$$

On all other boundaries except the target, set No slip conditions.

Outlet

We set a constant pressure at the outlet. The value of the pressure is

$$P_0 = 0 \quad (10)$$

Wetting walls

$$\mathbf{n} \cdot \mathbf{V} = 0 \quad (11)$$

$$\mathbf{F}_{wall} = \sigma(\mathbf{n} - \mathbf{n}_{int} \cos(\theta_w))\delta - \frac{\mu}{\beta} \mathbf{V} \quad (12)$$

The movement of droplets was based on the modification of contact angle θ_w in our simulation.

3.4 Numerical Results and Analysis

Numerical results of cutting process on different electrodes were analysed. Figure 4(a) shows the cross section outline of droplet at the initial moment and this outline is a regular circle; Figure 4(b) is the outline when voltage were applied, and TCL has now diffused.

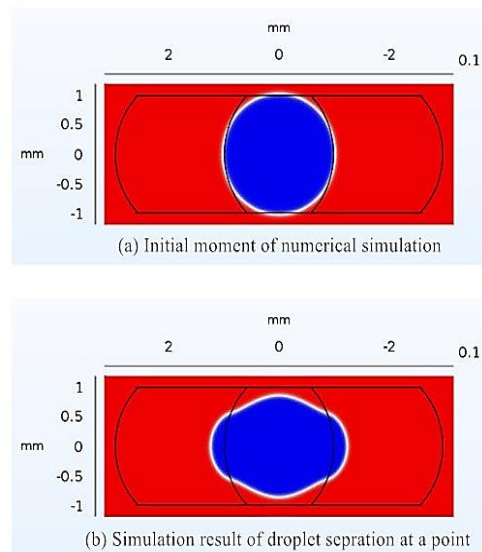


Fig. 4. Numerical simulation of droplet cutting.

The angle α in Fig.5 is a parameter for measuring the effective TCL of droplet. The larger the value of α , the larger the TCL and the greater the EWOD tension. It can be seen that the value of α on crescent electrode is larger than that on square electrode at the same time. Taking the crescent electrode ($A=1.41$) and the square electrode as examples. Initially, no voltage was applied, $\alpha=14^\circ$ in Fig. 5(a), and $\alpha=26^\circ$ in Fig. 5(d). Then, when the voltage was applied to the electrodes, α became larger, and when $t = t_1$, α increased to 21° in Fig. 5(a), and α increased to 30° in Fig. 5(d). When $t = t_2$, $\alpha=26^\circ$ in Fig. 5(a) and $\alpha=35^\circ$ in Fig. 5(d), α reached the maximum value at this time. Thereafter, the droplet started to shrink, and α gradually decreased. When $t = t_3$, $\alpha = 25^\circ$ in Fig. 5(a) and α

$= 29^\circ$ in Fig. 5(d). Finally, the cutting was completed in Figure 5(d) when $t = t_4$ as the droplet continued to shrink.

By analyzing the numerical results of square electrode and crescent electrode, it could be found that the cutting effect of the crescent electrode was better than that of the square electrode, and the cutting effect of crescent electrode was best when $A = 1.41$, which was because the effective TCL of droplet on square electrode changed more slowly than that of crescent electrode as the cutting time increased. Hence, the TCL and the EWOD tension of crescent electrode were larger than that of square electrode at the same time.

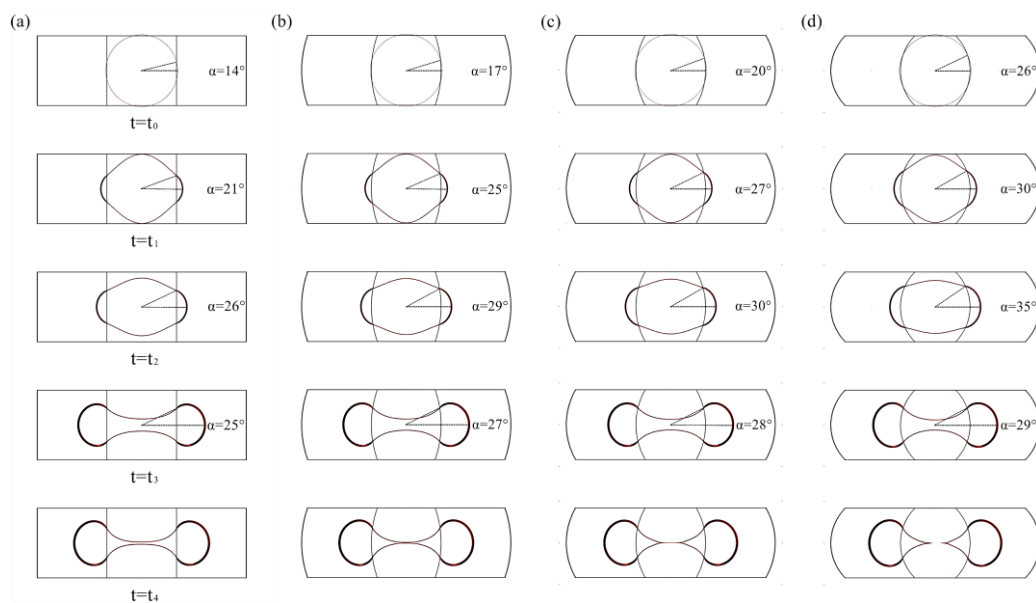


Fig. 5. Numerical results of cutting effect on different electrode shapes: (a) Square electrode; (b) Crescent electrode ($A=3$); (c) Crescent electrode ($A=2$); (d) Crescent electrode ($A=1.41$).

4. RESULTS AND DISCUSSION

4.1 Device Fabrication

We designed and fabricated four digital microfluidic chips with different structures, the electrode spacing was 30 microns. The major fabrication process steps of EWOD chips were shown in Fig. 6. Briefly, the photoresist was spin-coated on the substrate, and the electrode shape was etched onto the substrate by photolithography, thereafter, the desired electrode was obtained by sputtering and peeling. After this fabrication, SU8 was spin-coated as dielectric layer and Teflon was spin-coated as hydrophobic layer to achieve the bottom plate.

4.2 Experimental Tests

The signal during experiment was provided by the programmable power supply, the frequency was

fixed at 500 Hz, and the movement of droplet was recorded by CCD camera. In the experiment, a certain volume of deionized water was placed on the bottom plate of chip with a micro-syringe, and then the top and bottom plates were combined with a double-sided tape to form a "sandwich" structure. Figure 7 is the video sequences of 1 μ L droplet cutting.

Figure 8 shows the minimum voltage required for droplet cutting of different volumes. It can be seen that the minimum cutting voltage tends to increase as the droplet volume increases, and the larger the droplet volume, the larger the cutting voltage.

When the droplet volume was 0.8 μ L, the minimum cutting voltage for square electrode was 50V, while the minimum cutting voltages of three crescent electrodes were 47, 43 and 40V, respectively. The minimum cutting voltage of three crescent electrodes were 6%, 14%, 20% lower than that of

square structures, respectively. When the droplet volume increased to 1.8 μ L, the minimum cutting voltages of four electrodes were 72, 69, 66 and 62 V, respectively, and, the minimum cutting voltage of three crescent electrodes were 4.2%, 8.3%, 13.9% lower than that of square electrode, respectively.

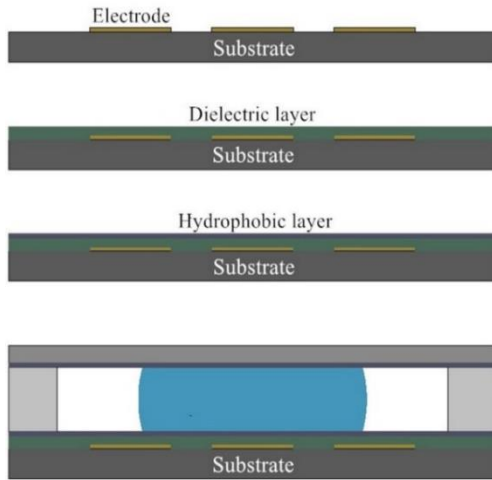


Fig. 6. Illustration of major fabrication process steps of chip based on EWOD.

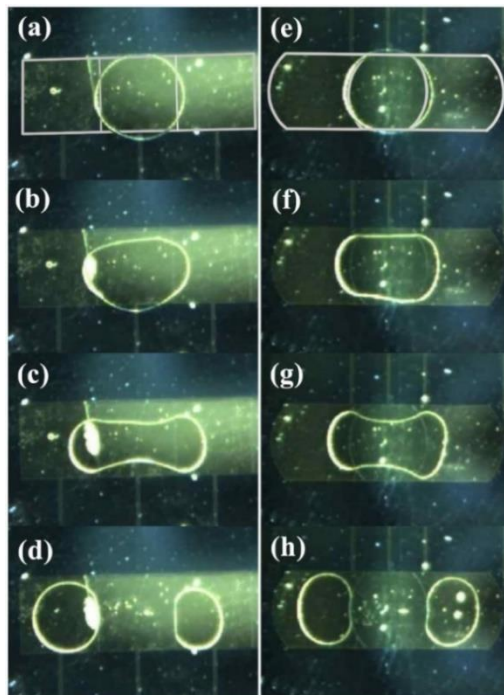


Fig. 7. Top view of video sequences of droplet separation on two kinds of splitting electrodes.

Thus it can be seen that the cutting voltage increases as the droplet volume increases, however, the minimum cutting voltage on crescent electrode is lower than that of square electrode regardless of the droplet volume. Furthermore, the minimum voltage required for cutting on crescent electrode ($A=1.41$)

is the smallest between four structures at the same time.

Figure 9 is the times of successful droplet cutting at different channel heights. It can be seen that the success rate is high and the difference between several chips is small when channel height is less than 100 μ m. When channel height is greater than 100 μ m, the success rate reduced, however, the rate of crescent electrode is greater than that of square electrode and the success rate of crescent electrode ($A=1.41$) is highest at any channel heights.

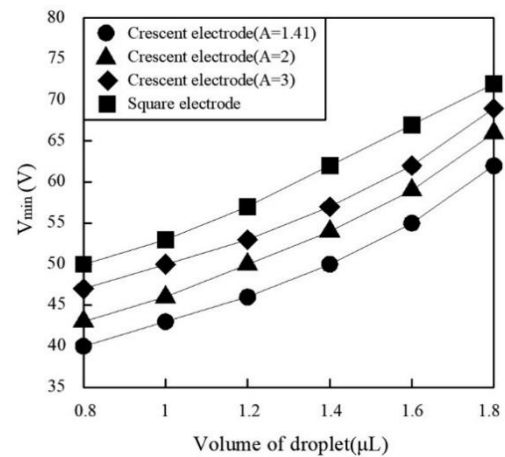


Fig. 8. Relationship between droplet volume and minimum cutting potential.

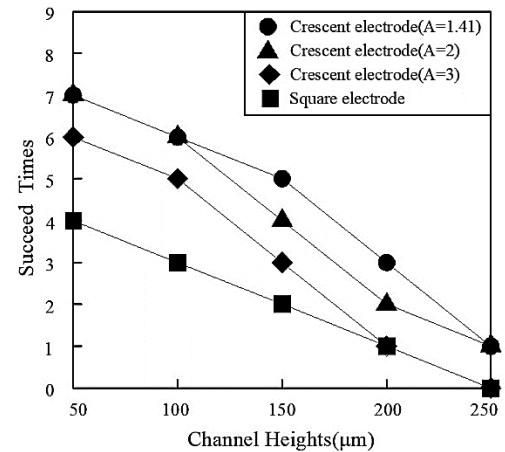


Fig. 9. Times of successful separate the droplet at different channel heights (every 10 times).

Numerical study and experimental result reveal that droplet can be split at lower voltages on crescent electrode, and the crescent electrode ($A=1.41$) has the best cutting effect among the four chips. And, the success rate of droplet cutting on crescent electrode at different channel heights is higher than that of square electrode under the

same conditions.

5. CONCLUSION

In this paper, we design four electrodes with different structures according to the relationship between the EWOD tension and the TCL of droplet. The effects of droplet cutting on these four electrodes were studied by numerical simulation and experiment. The results reveal that the crescent electrodes can decrease the applied voltage for droplet cutting, and the success rate of droplet cutting on crescent electrode at different channel heights is higher than that of square electrode. Therefore, the crescent electrode of digital microfluidic chip are conducive to the split of droplets.

ACKNOWLEDGMENT

Authors acknowledge financial support from the Major projects of Natural Science Research in Universities of Jiangsu Province of China (17KJA460008) and Natural Science Foundation of Jiangsu Province of China (BK20171215).

REFERENCES

- Choi, K., A. H. C. Ng, R. Fobel and A. R. Wheeler (2012). Digital microfluidics. *Annual Review of Analytical Chemistry* 5, 413-440.
- Fouillet, Y., D. Jary, C. Chabrol P. Claustre and C. Peponnet (2008). Digital microfluidic design and optimization of classic and new fluidic functions for lab on a chip systems. *Microfluidics and Nanofluidics* 4, 159-165.
- Haeberle, S. and R. Zengerle (2007). Microfluidic platforms for lab-on-a-chip applications. *Lab on a Chip* 7, 1094-1110.
- Jagath, B. N. N. Y., M. M. Nahar and H. Moon (2017). Accurate, consistent, and fast droplet splitting and dispensing in electrowetting on dielectric digital microfluidics. *Micro and Nano Systems Letters* 5(1), 24 (10 pp.)
- Jebrail, M. J., M. S. Bartsch and K. D. Patel (2012). Digital microfluidics: a versatile tool for applications in chemistry, biology and medicine. *Lab on a Chip* 12, 2452-2463.
- Jong, H. C. and J. James (2011). Twin-plate electrowetting for efficient digital microfluidics. *Sensors and Actuators* 160, 1581-1585.
- Karniadakis, G. E. and A. Beskok (2001). *Micro Flows: Fundamentals and Simulation*. Springer-Verlag.
- Mark, D., S. Haeberle, G. Roth, F. vonStetten and R. Zengerle (2010). Microfluidic lab-on-a-chip platforms: requirements, characteristics and applications. *Chemical Society Reviews* 39, 1153-1182.
- Mugele, F. and J. C. Baret (2005). Electrowetting: from basics to applications. *Journal of Physics: Condensed Matter* 17, 705-774.
- Olsson, E. and G. Kreiss (2005). A conservative level set method for two phase flow. *Journal of Computational Physics* 210, 225-246.
- Osher, R. and R. Fedkiw (2003). *Level Set Methods and Dynamic Implicit Surfaces*. Springer-Verlag.
- Panton, R. L. (1996). *Incompressible Flow*, 2nd ed. Wiley.
- Rajabi, N. and A. Dolatabadi (2010). A novel electrode shape for electrowetting-based microfluidics. *Colloids and Surfaces A: Physicochemical and Engineering Aspects* 365(1-3), 230-236.
- Samad, M. F., A. Z. Kouzani, M. M. Rahman, K. Magniez and A. Kaynak (2015). Design and fabrication of an electrode for low-actuation-voltage electrowetting-on-dielectric devices. *Procedia Technology* 20, 20-25.
- Shen, H. H., S. K. Fan, C. J. Kim and D. J. Yao (2014). EWOD microfluidic systems for biomedical applications. *Microfluid Nanofluid* 16, 965-987.
- Walker, S. W. and B. Shapiro (2006). Modeling the fluid dynamics of electrowetting on dielectric (EWOD). *Journal of Microelectromechanical Systems* 15(4), 986-1000.
- Xu, X. W., L. N. Sun, L. G. Chen, Z. Z. Zhou, J. J. Xiao and Y. L. Zhang (2014). Electrowetting on dielectric device with crescent electrodes for reliable and low-voltage droplet manipulation. *Biomicrofluidics* 8(6), 064107.
- Yue, P. T., J. J. Feng, C. Liu and J. Shen (2004). A diffuse-interface method for simulating two-phase flows of complex fluids. *Journal of Fluid Mechanics* 515, 293-317.